Metal-insulator transitions in $NdNiO_3$ thin films

G. Catalan, R. M. Bowman, and J. M. Gregg*
Condensed Matter Physics & Material Science Research Division, School of Mathematics and Physics, Queens University of Belfast, Belfast BT7 1NN, United Kingdom
(Received 9 November 1999; revised manuscript received 28 January 2000)

We present a study of the crystallography and transport properties of $NdNiO_3$ thin films, grown by pulsed-laser deposition, on a variety of substrates and with a range of thicknesses. Results highlight the importance of epitaxy, and show that $NdNiO_3$, with a sharp metal-insulator phase transition, can be fabricated without the need for high-pressure processing. The conductivity of the nickelate films was found to be well described by a linear sum of activated transport and Mott's variable range hopping in the entire measured temperature range of the semiconducting state, and this description was also found to provide an accurate fit for previously published transport properties of bulk ceramics. The transition was subsequently modeled using a percolative approach. It was found that the temperature of the metal-insulator phase transition, in both our films and in bulk, corresponded to a critical percolation threshold where the volume fraction of the semiconducting phase (V_s) was $\frac{2}{3}$, as expected for a three-dimensional cubic lattice. For the thinnest films grown on $NdGaO_3$, a possible crossover to two-dimensional percolation was indicated by $V_s=\frac{1}{2}$.

INTRODUCTION

Rare-earth nickelates have the generic formula $RNiO_3$ (where R is a lanthanide rare earth), and belong to the perovskite structural family. Compounds in which the rare earth is smaller than lanthanum are orthorhombically distorted at room temperature, and display a first-order metal-insulator (MI) phase transition.[1] Evidence suggests that the critical temperature of the phase transition (T_{MI}) is dependent on the Ni-O-Ni bond angle: straightening the angle stabilizes the metallic state over the semiconducting one, lowering T_{MI}. This can be achieved by increasing rare-earth radius or by applying external hydrostatic pressure.[1–5] In general there is only a slight volume reduction, and no observable structural change across the semiconductor-metal transition,[6] although it should be noted that in $YNiO_3$ a symmetry change has been detected between $Pbnm$ and $P2_1/n$ space groups.[7]

The low-temperature state of nickelates is generally classified as a low-Δ charge-transfer semiconductor.[8,9] The transition to a high-temperature metallic state is believed to be caused by gradual closing of the band gap between the oxygen p and the nickel d orbitals across the Fermi level. Conduction then proceeds according to $d_i^{3+}p_j^{2-}\leftrightarrow d_i^{2+}p_j^{1-}$, with the charge carriers being heavy electrons in both the metallic and semiconducting states.[10] Although the expected Jahn-Teller distortion of the NiO_6 octahedra has not been directly observed, recent oxygen isotope exchange experiments suggest that indeed Jahn-Teller polarons are present even in the metallic phase.[11] Nickelates also show unique low-temperature magnetic ordering: Ni ions, in ''ferromagnetic planes'' perpendicular to the $[111]_{pseudocubic}$, couple in the sequence $(++--++--)$.[12] Although the Néel temperature (T_N) coincides with T_{MI} for $R=$Pr and Nd, the magnetic ordering in the rest of the series is independent from the MI transition,[1] confirmed by the fact that magnetic fields have no significant influence over transport properties.[2,13]

However, some fundamental aspects of the transport properties of nickelates, particularly in the low-temperature semiconducting state,[13,14] are still not fully understood. For example, to date no simple function has been capable of fitting the entire temperature range of the semiconducting state, and questions such as whether the charge-transfer gap is itself a function of temperature,[10] or the possible participation of Mott's variable range hopping (VRH) in the conductivity,[13] remain open.

Another issue concerns the difficulty in synthesizing nickelates with a sharp MI transition: the synthesis of nickelates with good MI switching properties requires the application of high pressures (~200 bar) of oxygen at relatively high temperatures (~1000 °C). Nickelates made under ambient pressure show only a marginal transformation behavior. Since high processing pressures are not easily attainable, they represent an important obstacle for widespread nickelate research. This paper addresses these two issues, and is divided into two main sections.

(i) *Synthesis*: the specimens studied in this work were fabricated by pulsed laser deposition (PLD). This fabrication method produced $NdNiO_3$ with a sharp MI transition without the need for high-pressure processing. A description and rationalization of the crystallographic and transport properties of the films is presented.

(ii) *Modeling*: A model for the semiconducting state of $NdNiO_3$, applicable to both thin films and ceramics, was found. This was then used to characterize the percolative transitions in the films.

I. SYNTHESIS

Crystallization of perovskite nickelates requires the nickel to adopt the relatively unstable Ni^{3+} valence state. Demazeau *et al.*[15] were the first to report successful nickelate synthesis using high temperature-high pressure conditions: R_2O_3, NiO, and $KClO_3$ were reacted together in a sealed platinum capsule at 950 °C, and thermal decomposition of the chlorate produced in-situ oxygen pressures of 60 kbar. Vassiliou *et al.*, on the other hand, reported $PrNiO_3$ and $NdNiO_3$ prepared by sol-gel methods, with typical firing conditions of ~600 °C and atmospheric pressure.[16] Although

other variations on the sol-gel route have been described,[17] nickelates prepared following low-pressure methods tend to be oxygen deficient, and show only marginal transformation.

Lacorre *et al.* used high-temperature–high-pressure synthesis, reacting oxides at ~1000 °C and ~200-bar O_2.[1] To date, only specimens prepared under these conditions have shown the characteristic sharp first-order MI transition. Although thin films with good switching properties have been made by sputtering, a high-pressure post-anneal was still required to achieve optimum switching characteristics.[18]

Recently the authors established that PLD could be used to grow thin films with as-grown switching characteristics comparable to those of nickelates processed at high pressures.[19] The details of the growth process and the analysis of results are presented below.

A. Experiment

The thin films of $NdNiO_3$ were grown from an oxide ceramic target onto single-crystal substrates of {100} MgO, {100} $SrTiO_3$ (STO), {110} $NdGaO_3$ (NGO), and {100} $LaAlO_3$ (LAO), with a KrF excimer laser (Lambda Physik COMPex 205*i*, $\lambda = 248$ nm). Typical deposition conditions were 0.15-mbar O_2, 675 °C and with an energy density of ~1.5 J/cm^2 at a pulse frequency of 10 Hz. Typical deposition times of 15 min yielded film thicknesses of several hundred nm. Films of reduced thickness were also fabricated to study the effect of epitaxial strain on transport properties.

The out-of-plane lattice periodicity of all the films was deduced from conventional θ-2θ x-ray diffraction (XRD) on a Siemens D5000 diffractometer using Cu $K\alpha$ radiation. Information on the in-plane crystallography was obtained from plan-view transmission electron microscopy (TEM). A Philips 400T microscope was used. TEM sample preparation was performed using standard grinding and milling techniques.

dc resistance was measured as a function of temperature for all samples using a conventional four-probe technique (HP 34401 A dc multimeter) and a closed-cycle cryostat (CTI cryogenics M22). Resistance was measured on both cooling and heating in a temperature range of 12–300 K. The measuring currents were automatically changed by the multimeter to ensure linearity in all resistance ranges; these were 1 mA for $R < 1\ \text{k}\Omega$, 0.1 mA for $1\ \text{k}\Omega < R < 10\ \text{k}\Omega$, and 10 μA for $10\ \text{k}\Omega < R < 100\ \text{k}\Omega$. The temperature was controlled by a Lakeshore 330 temperature controller, with a ramp rate of 3 K/min.

B. Results and discussion

1. Crystallography

$NdNiO_3$ films grown on MgO showed relatively poor crystallinity with only $\{110\}_{\text{pseudocubic}}$ and $\{200\}_{\text{pseudocubic}}$ reflections apparent [Fig. 1(a)]. These two reflections have been observed to be the most intense in randomly distributed powder diffraction patterns.[1] X rays would therefore indicate that films grown on MgO are likely to be randomly oriented. Subsequent plan-view TEM investigation largely supports this interpretation, as diffraction images [Fig. 2(a)] show limited in-plane orientation and no systematic absences.

In contrast, films grown on STO, LAO, and NGO show strong preferential orientations with $\{100\}_{\text{pseudocubic}}$ parallel to the substrate surface [Figs. 1(b)–1(d)]. TEM, performed on a film grown on NGO [Fig. 2(b)], also indicates a high degree of in-plane orientation. The diffraction pattern shows a doubling of the cell periodicity along one of the in-plane axes, consistent with a $NdNiO_3$ orthorhombic in-plane *c* axis. This orientation minimizes the total mismatch strain on NGO. On the whole, these results suggest coherent or semicoherent growth of films on STO, NGO, and LAO, and incoherent growth on MgO.

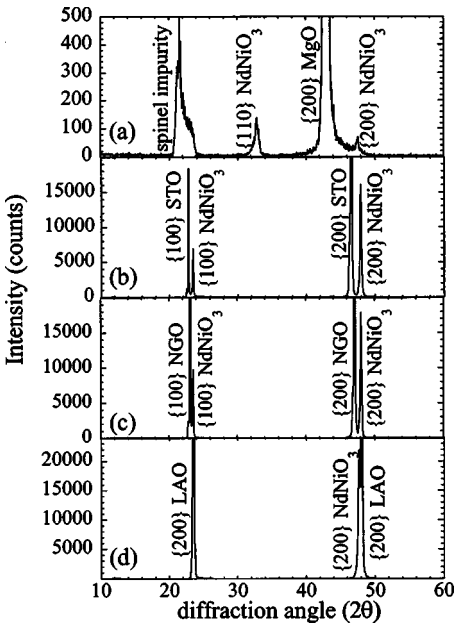

FIG. 1. θ-2θ XRD scans for films grown on (a) MgO, (b) STO, (c) NGO, and (d) LAO. Films grown on STO, NGO, and LAO show a preferential orientation $\{100\}_{\text{pseudocubic}}$ parallel to the substrate, suggesting epitaxy. Films grown on MgO are consistent with random orientation. The spinel impurity originates from the substrate.

Table I shows the out-of-plane perovskite lattice parameter of the films as a function of substrate as measured by XRD. The lattice parameter on LAO is relatively undistorted from bulk values [$c = 3.807$ Å (Ref. 1)], owing to the relatively small lattice mismatch. The out-of-plane lattice parameters on STO and NGO are below bulk values, but full co-

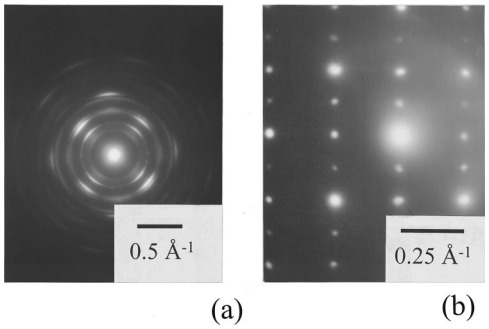

FIG. 2. Plan-view TEM selected area diffraction from a film grown on MgO (a) and NGO (b). Both diffraction patterns are consistent with a perovskite structure, but whereas films on MgO show a limited preferential orientation, films on NGO are coherently oriented with an orthorhombic in-plane *c* axis, as indicated by the doubling of the real-space periodicity along one of the axes.

TABLE I. Substrate pseudocubic lattice parameters, lattice mismatch between substrate and $NdNiO_3$ bulk ceramics (extracted from Ref. 1), and film out-of-plane periodicity deduced from θ-2θ XRD scans.

	MgO	STO	NGO	LAO
Substrate pseudocubic lattice parameter (Å)	4.20	3.89	3.86	3.79
Substrate-bulk nickelate mismatch	10.2%	2.10%	1.31%	−0.5%
Film's out-of-plane pseudocubic lattice parameter (Å)	3.830 ±0.005	3.797 ±0.005	3.784 ±0.005	3.806 ±0.005

herence and volume conservation of the nickelate unit cell would predict the out-of-plane lattice parameter to be more contracted for films grown on STO than on NGO. As this is not the case, the results suggest that films grown on STO are likely to be less coherent than those grown on NGO.

2. Switching characteristics

Figure 3 shows typical curves for the resistance as a function of temperature for films grown on different substrates. To allow a precise comparison of behaviors, we have defined the following parameters.

Metal-insulator transition temperature (T_{MI}): the temperature of the maximum in the plot $-d(\ln R)/dT$ against T on heating.[2]

Transition hysteresis: the difference between T_{MI} on heating and on cooling.

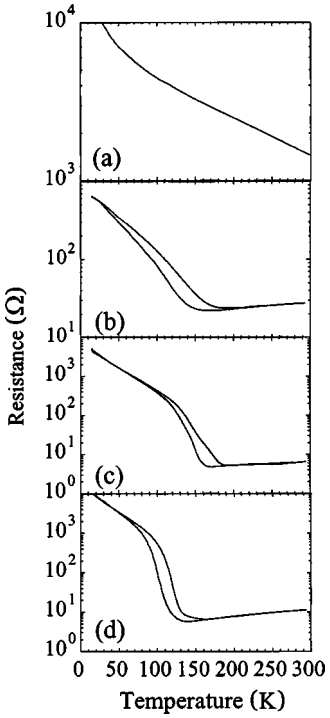

FIG. 3. Resistance as a function of temperature for $NdNiO_3$ films grown on (a) MgO, (b) STO, (c) NGO, and (d) LAO. The transition sharpness improves as the substrate-film lattice mismatch decreases.

TABLE II. Properties of the metallic state and the MI phase transition for $NdNiO_3$ films grown on different substrates. Typical bulk ceramic values have been extracted from Refs. 2 and 10 to allow a comparison.

Substrate	T_{MI}/K	Hysteresis/K	Sharpness	Resistance change	Metallic quality
$SrTiO_3$	130	20	0.025	~20	1.7×10^{-3}
$NdGaO_3$	170	25	0.07	~150	2.7×10^{-3}
$LaAlO_3$	120	20	0.2	~500	3.3×10^{-3}
Bulk	195	4	0.7	~1000	3.5×10^{-3}

Transition sharpness: peak value of $-d(\ln R)/dT$ against T on heating.

Resistance change across transition: ratio of the resistances at the beginning and end of the hysteresis in the resistance-temperature plot.

Quality of the metallic state: normalized resistance slope at room temperature $(1/R\, dR/dT@300\,\mathrm{K})$.[10]

These parameters are summarized for each of the films in Table II along with those characteristics of bulk samples (except for films grown on MgO, which are semiconducting at all measured temperatures). Three of the parameters—transition sharpness, resistance jump, and normalized resistance slope—show more bulklike behavior as the lattice mismatch is reduced. Hysteresis across the transition is relatively constant and greater than that observed in bulk. T_{MI} increases from STO to NGO, but is dramatically reduced on LAO.

In all cases, the switching characteristics of the as-grown films were superior to those reported to date for ceramics fabricated by low-pressure techniques. The properties of the films grown on LAO are comparable to those sputtered and annealed under high pressure by DeNatale and Kobrin,[18] despite the fact that growth by PLD did not involve any post-deposition annealing. PLD is a relatively high-energy process compared to sputtering. Ionized plume species in PLD have an energy of the order of hundreds of eV,[20] and since the ionization potential of Ni^{3+}, required to form $NdNiO_3$, is 35.16 eV,[21] it seems likely that PLD is capable of producing Ni^{3+} during deposition, making the later stage of high-pressure post-annealing unnecessary.

However, excitation of the species within the plume is not the only factor required for the production of films with good switching characteristics. Films grown on MgO are incoherent, and do not display any MI transition, and in general, as seen above, the properties of the transition improve as the lattice mismatch is decreased. It is thus necessary that two factors act simultaneously: (i) A high-energy deposition process (capable of producing Ni^{3+} ions in the plume). (ii) A good epitaxial match between the film and substrate.

One general feature of the MI transition of the nickelate films is that T_{MI} is significantly lower than for bulk ceramics. This cannot be attributed to an oxygen deficiency, as recent work on sol-gel-derived samples indicates that oxygen vacancies raise T_{MI}, rather than lowering it.[22,23] DeNatale and Kobrin[18] argued that depression of T_{MI} in thin films is a result of epitaxial strain. This possibility is explored in Sec. I B 3.

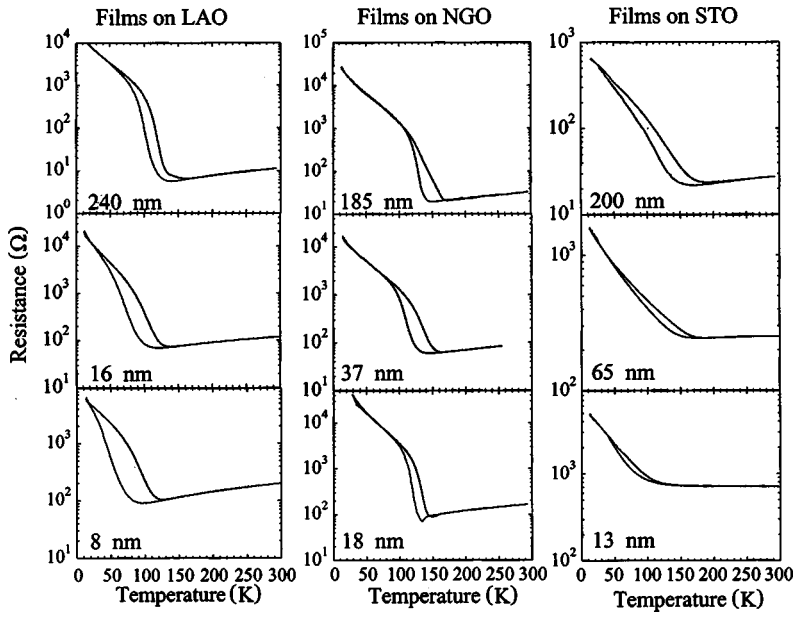

FIG. 4. Resistance as a function of temperature for films of different thickness grown on LAO, NGO, and STO. T_{MI} decreases for thinner films, suggesting strong epitaxial strain effects.

3. Epitaxial strain effects on transport properties

Films of reduced thickness were grown on STO, NGO, and LAO substrates. When the film thickness is reduced, the relative impact of the strain generated at the film-substrate interface becomes increasingly important, and thus the changes in related properties become more obvious. Film thickness was reduced by decreasing the deposition time from 15 min down to 30 s. The thickness of the resulting films ranged from ~550 nm down to ~8 nm.

Figure 4 shows the evolution with thickness of the resistance as a function of temperature for films grown on STO, NGO, and LAO, respectively. There is a marked difference between the behavior of films grown on STO and those grown on NGO and LAO. The quality of the metallic state for films grown on STO substrates decreases on reducing the film thickness to such an extent that, for the thinnest films, the normalized resistance slope at room temperature becomes negative, and the ''metal-insulator'' transition is only signaled by hysteresis in the resistance curves, with the distinction between the ''metallic'' and the semiconducting states being marginal. Films grown on NGO and LAO, on the other hand, show a clear MI phase transition in all cases.

Thicker films grown on NGO display a double peak in $-d(\ln R)/dT$ against T (Fig. 5). As the thickness decreases, the relative height of the double peaks changes, and for the thinnest films only one of the peaks is evident. This anomalous behavior does not appear in the films grown on LAO.

The origin of this double peak is uncertain. One possible explanation is that the nature of strain in films grown on NGO can decouple the magnetic transition from the metal-insulator one. Certainly lattice distortion in nickelates in which the rare earth is smaller than Nd decouples T_N from T_{MI},[1] and anomalies in resistance associated with the Néel temperature[24] are observed.[25] However, the double peak would then be expected in the thinner, more strained films, which is not the case.

Another possible explanation is that the epitaxial strain for films grown on NGO exceeds the critical elastic energy necessary to produce systematic misfit dislocations. The elastic strain energy in the films is proportional to the lattice mismatch and to the thickness, and consequently there is a critical thickness (t_c) above which the elastic energy may be sufficient to produce dislocations.[26] Films thicker than t_c may therefore show two distinct regions: one closer to the substrate and relatively dislocation free; and one farther from the substrate, in which the dislocations alleviate the epitaxial strain. It is conceivable that these two regions would have two different transition temperatures: lower for the dislocation-free region, in which the whole film experiences the maximum strain; and higher for the upper region, in which the strain has been relaxed. As the film thickness is reduced, the relative importance of the two regions will shift towards the dislocation-free one, and eventually films thinner than t_c will only show one transition temperature and a sharp resistance change, which is the trend observed in Fig. 5.

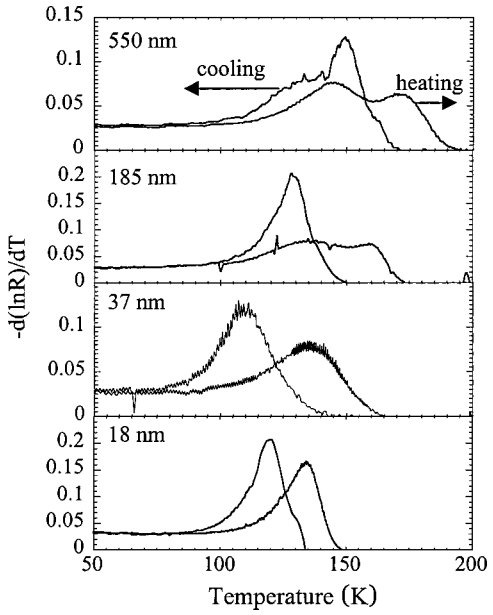

FIG. 5. Evolution as a function of thickness of the peak in $-d(\ln R)/dT$ against T for films grown on NGO. The double peak of the thicker films disappears in the thinner ones.

However, the critical thickness inferred from transport properties is much greater than that estimated using the Mathews-Blakeslee formula[26–28]

$$\varepsilon_m = \frac{[b_x^2 + b_y^2 + (1-v)b_z^2]}{8\pi(1+v)b_x} \frac{1}{t_c} \ln \beta \frac{t_c}{r_0}, \tag{1}$$

where r_0 is the pseudocubic perovskite lattice parameter of the film, (b_x, b_y, b_z) is the Burgers displacement vector of the dislocation, v is the Poisson ratio of the film, β is a dimensionless constant, and ε_m is the lattice mismatch between substrate and film. Typical values for perovskites are $v = \frac{1}{4}$ and $\beta \approx 4$,[28] and perovskite films on perovskite substrates tend to show dislocations with pseudocubic $\langle 100 \rangle$ Burgers vectors.[28] Substituting these values in the above formula yields a critical film thickness of $\sim 10 r_0$ on NGO, and $\sim 30 r_0$ on LAO, as opposed to the observed values of $\sim 100 r_0$ for NGO and $> 600 r_0$ for LAO, and therefore the appropriateness of this ''double-layer'' hypothesis remains to be clarified.

One common feature was observed in all films, regardless of the substrate: T_{MI} decreases as thickness is reduced. The reduction in T_{MI} and the decrease in the resistivity of the semiconducting state can certainly be rationalized in terms of epitaxial strain. Strain has a direct impact on the lattice parameters of the $NdNiO_3$ films, and consequently on the Ni-O-Ni bond angle. Straightening out this angle increases orbital overlap, stabilizing the metallic phase and decreasing T_{MI}.

For films grown on NGO and STO, the in-plane tensile strain straightens the bond angle parallel to the substrate. Intuitively, however, the in-plane compressive strain induced by growth on LAO would not be expected to produce this bond straightening.

A subtler effect, however, may be responsible: LAO substrates are rhombohedral, and thus an increase in the nickelate film in-plane symmetry is expected under coherent growth. An estimate of the Ni-O-Ni bond angles can be obtained using Hayashi's formula[29]

$$\theta = 135 + \sqrt{13.4(\theta_0 - 135)}, \tag{2}$$

where $\cos \theta_0 = 1 - 2a^2/b^2$, and a and b are the orthorhombic lattice parameters of $NdNiO_3$. If a and b grow in-plane (minimum coherent strain growth condition), then $a \approx b$, and, therefore, $\theta_0 \approx 180°$, which yields an in-plane Ni-O-Ni bond angle of 159.6°, wider than the measured bond angle for undistorted $NdNiO_3$ ceramics at room temperature: $\theta = 157.1°$.[6] Furthermore Canfield *et al.*[2] have related the bond angle to T_{MI}: for the T_{MI} observed in the thinnest films grown on LAO (~100 K), a bond angle of ~159° would be expected, in good agreement with the above calculations.

II. MODELING OF THE SEMICONDUCTING STATE AND PERCOLATIVE ASPECTS OF THE MI TRANSITION

It has been proposed that in the hysteretic zone of the transition, a binary mixture of metallic and insulating regions coexist; the relative ratios of metallic and insulating material change with temperature, determining the dynamics of the phase transition.[10] Within this context, the effective medium approximation consists of replacing a random distribution of metallic and insulating bonds by a homogeneous lattice in which every bond has the same conductance G_e. This conductance is given by[30]

$$\frac{P_m(G_e - g_m)}{g_m + (D-1)G_e} + \frac{P_s(G_e - g_s)}{g_s + (D-1)G_e} = 0 \tag{3}$$

in a cubic lattice with $2D$ nearest neighbors (D is the dimensionality of the system). P_m and P_s are the probability of a bond being metallic or semiconducting (in a homogeneous medium, the volume ratio of metallic and insulating phases in the mixture), and g_m and g_s are the corresponding conductivities of such bonds. Two observations can be made: first, for $D = 3$ this result is the same as that corresponding to spherical particles in an homogeneous medium, as assumed by Granados *et al.*;[10] second, one can relate the observed peak in $-d(\ln R)/dT$ against T to a percolation threshold: to a first approximation, let $g_s = 0$. The conductivity of the medium will then be given by

$$G_e = \frac{g_m(DP_m - 1)}{D-1} = 1/R; \tag{4}$$

therefore,

$$-\frac{\partial \ln R}{\partial P_m} \propto \frac{1}{DP_m - 1}. \tag{5}$$

Thus, there is a singularity in $-\partial \ln R/\partial P_m$ when $P_m = 1/D$. If the probability of a bond being metallic changes with temperature, as in the nickelates, then an anomaly should be expected in $-d(\ln R)/dT$ when the temperature is such that $P_m = 1/D$. Thus the temperature of the observed peak in the graphs of $-d(\ln R)/dT$ corresponds to that of the critical threshold for the loss of connectivity in the percolation network.

Following the approach of Granados *et al.*,[10] $g_m(T)$ is approximated by extrapolating the conductance of the film well above T_{MI}, $g_s(T)$ is fitted by the conductance of the semiconducting phase below the closing of the hysteresis, and $G_e(T)$ is the actual measured conductance of the films in the mixed state. Assuming that the probability of a bond being metallic or semiconducting is equal to the relative volume of the metallic and semiconducting states respectively, the substitutions $P_s = V_s$ and $P_m = 1 - V_s$ can be made in formula (3); the relative volume of semiconducting phase within the nickelate film, $V_s(T)$, can then be extracted from Eq. (3).

The conductivity of the metallic state ($g_m(T)$) is easily fitted by a linear regression; the description of the semiconducting state is more complex, but is essential for the determination of $V_s(T)$, as described above. This is dealt with in Sec. II A.

A. Fitting of the semiconducting state

In previous work, attempts to fit the semiconducting state to simple activated behavior ($\log \sigma \sim 1/T$) failed, as there is a steady curvature in the Arrhenius plot.[2,13,10] In order to explain the curvature, it was proposed that the activation energy is itself temperature dependent, being at a minimum

near the transition and increasing as the temperature is decreased. It has also been suggested[13] that at lower temperatures the conduction could be dominated by Mott's variable-range hopping [VRH, $\log \sigma \propto T^{-1/4}$ (Ref. 31)]. However, this fit appears to be accurate only below 30 K. Power laws have also been proposed for oxygen-deficient, sol-gel-derived samples.[22] To data, no fit based on a single conduction mechanism seems to accurately describe transport behavior over the entire semiconducting temperature range. An accurate fitting of the semiconducting state, and an extrapolation of this fit to determine $V_s(T)$ in the mixed region of the phase transition, therefore presented a problem.

Mallik *et al.*[13] observed that the semiconducting state could be divided into regions with apparently different transport behaviors. One approach could therefore consist of dividing the semiconducting range into two parts, one below ~30 K, where VRH would account for the total conduction, and another between 30 K and the start of the transition, where a thermal activation law with a temperature-dependent gap would account for the transport. But this approach presents several problems.

(i) The splitting into two smaller ranges, and the number of parameters added in order to describe the temperature dependence of the gap, would ensure a good mathematical fit of the conductivity, without it being necessarily physically meaningful.

(ii) The origin of the temperature dependence of the gap has not been physically justified, nor has the actual existence of a sharp transition between conduction mechanisms. These assumptions are merely mathematically convenient.

(iii) To date, no specific formula has been offered to describe the actual temperature dependence of the gap and choosing a particular one in this context would also be arbitrary.

Instead, we propose that a better model for the semiconducting state in $NdNiO_3$ can be obtained by assuming a combination of more than one transport mechanism acting simultaneously throughout the entire temperature range, in this case VRH and activated behavior. A similar approach was used before in the nickelates, where a mixture of VRH and *metallic* conduction was postulated to model the transport properties of oxygen-deficient semiconducting $LaNiO_{3-\delta}$, providing a satisfactory fit in the temperature range 10–300 K.[32] The coexistence of various parallel conduction channels in a single material is not new, as semiconducting systems are often described in this way.[33] However, we feel that it is important to address two points: (i) why VRH should be expected to persist at relatively high temperatures in $NdNiO_3$, rather than abruptly disappear above 30 K; and (ii) why dual conduction approaches used for the description of doped semiconductors may be appropriate for $NdNiO_3$.

Electron-lattice interactions are thought to be very important in perovskite nickelates.[34] Optical measurements,[35] the oxygen-isotope exchange experiment,[11] and the dramatic effect of pressure[2,3] and/or strain[18,19] on the transport properties of nickelates leave little doubt about the importance of electron-lattice coupling in these compounds. The strength of the polaronic coupling means that scattering by phonons should be expected to play an important role in the transport properties. As has been pointed out,[36] a strong electron-phonon interaction is expected to promote VRH to relatively high temperatures. Further, Pollak *et al.*[37] showed that the traditional temperature limit for VRH, implied by $E_m = kT\xi_m$ (where ξ_m is the exponent of the critical percolation impedance in a random network, and E_m is the maximum energy difference between the Fermi level and the localized states involved in the hopping) was not a real limitation in percolative systems, because hopping was strongly biased toward sites much closer to the Fermi level than E_m.

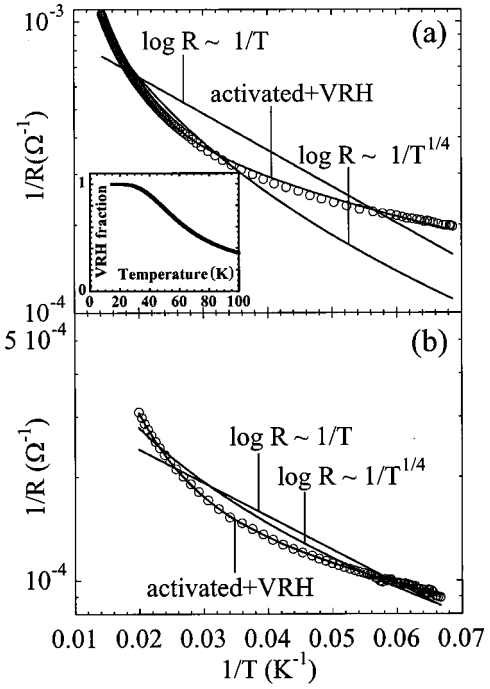

FIG. 6. Fits to the semiconducting state of $NdNiO_3$ films grown on (a) NGO and (b) LAO. The best fits correspond to a combination of activated conduction and VRH of the form $1/R = A\exp(-B/T^{1/4}) + C\exp(-D/T)$. Inset: hopping contribution to the total conductance, showing that the participation of VRH is important even at the higher temperatures, being completely dominant below $T \sim 35$ K.

A dual mechanism, in which activated behavior and VRH are the only terms, was demonstrated in doped semiconductors near the critical doping level for the crossover between metallic and semiconducting behavior.[33] Although $NdNiO_3$ is not a doped semiconductor, perovskite nickelates are compositionally very close to the crossover between metallic and semiconducting behaviors in the Zaanen-Sawatzky-Allen scheme.[8,9] Thus the semiconducting state of nickelates below T_{MI} would appear similar to that of a semiconductor near the critical doping regime, for which a dual conduction mechanism with a strong hopping contribution should be expected.

We therefore modeled the semiconducting state of $NdNiO_3$ as the direct sum of two terms (conductances acting in parallel), one arising from VRH and another from normal activated conduction with a constant (temperature-independent) activation energy:

$$\sigma \propto 1/R = A\exp(-B/T^{1/4}) + C\exp(-D/T), \qquad (6)$$

where A, B, C, and D are constants.

Figure 6 shows the Arrhenius plots for the semiconducting state of two typical films grown on LAO and NGO. To allow comparison, the curves have been fitted by VRH, ac-

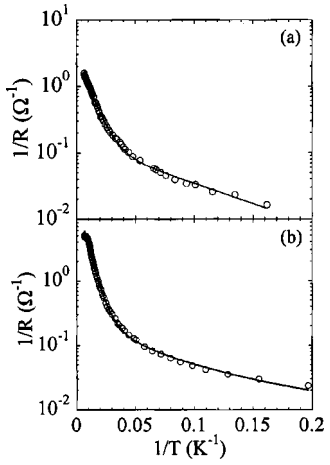

FIG. 7. The good fit to the semiconducting state (5–150 K) for bulk ceramics [data adapted from Refs. 13 (a) and 2 (b)] suggests that the dual conduction mechanism is a general feature of $NdNiO_3$.

tivated conduction, and a combination of both, to the temperature range between the lowest measured temperatures (12 K) and the beginning of the transformation (~90 K for films grown on NGO and ~50 K for films grown on LAO).

The fit that takes both phenomena into consideration is noticeably better, with correlation coefficients $r>0.999$. The coefficient D of the $1/T$ exponential corresponds to the band gap, and yields a consistent value around 200 K regardless of substrate and thickness. This is reassuring, as the corresponding activation energy (~17–20 meV) is in good agreement with the values found fitting the higher temperatures to an Arrhenius law.[2,10]

In order to illustrate to what extent VRH participates in the total conduction, we have plotted (inset in Fig. 6) the ratio between the VRH contribution to the fit and the total conductance. The result shows that participation of VRH in transport is significant even at relatively high temperatures. Importantly, for temperatures below ~35 K, VRH is virtually the only contribution to the total conductivity, which explains why VRH alone can provide a good fit below this temperature.[13]

In summary, the fit to the sum of both activated behavior and VRH is capable of accounting for the conduction behavior through the entire semiconducting range in our films, without the need for postulating either a temperature-dependent activation energy or different temperature regimes for each conduction mechanism.

It could be argued that a model involving the use of four fitting parameters is likely to produce a good mathematical fit for any well-behaved curve in the relatively limited temperature range considered (12–90 K). A good test for the validity of the model can therefore be obtained by expanding its temperature range. Although this is impossible to do in our films, as the purely semiconducting state only goes up to 90 K, the model can be tested for the semiconducting transport behavior of bulk ceramics as extracted from published literature. Figure 7 shows the Arrhenius plots for the semiconducting states of two different samples extracted from Refs. 2 and 13. The conductivity of the semiconducting state of these samples was fitted with formula (6) in the temperature range 5–150 K. Again, the dual conduction mechanism

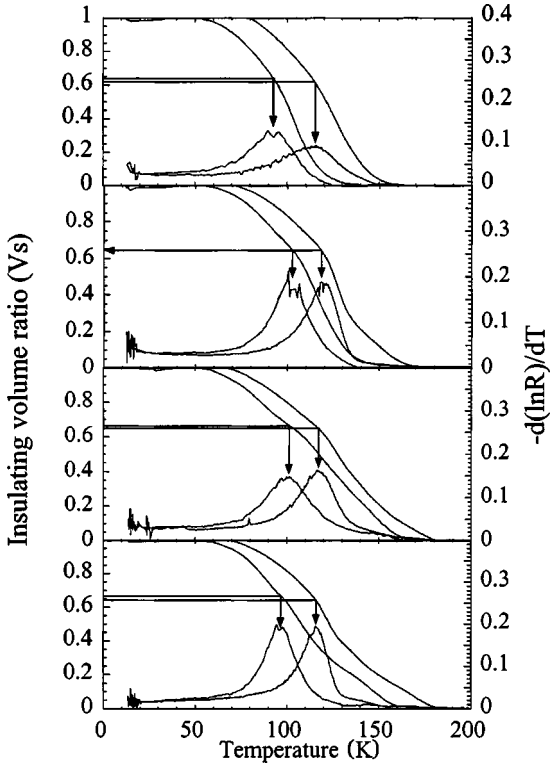

FIG. 8. Volume fraction of the insulating phase $V_S(T)$ and $-d(\ln R)/dT$ as a function of temperature on heating and cooling for films of standard thickness (~200 nm) grown on LAO. The peak that signals T_{MI} always corresponds to a volume fraction $V_s \cong 2/3$, the percolation threshold of a three-dimensional cubic lattice.

seems to provide a good fit. We therefore think that this is a genuine, general feature of the semiconducting state of $NdNiO_3$, and not a spurious effect that may be attributed to defects in the films studied here, or a mathematical artifact resulting from analysis on limited temperature ranges.

At the very least, the fitting approach used allows a confident extrapolation of the transport behavior associated with the semiconducting component beyond the onset of the percolative transition in $NdNiO_3$. It therefore provides an effective method for the determination of $V_s(T)$, leading to a further possible analysis of the transition outlined below.

B. Percolative effects on the transition: dimensionality of the model

Once the metallic and semiconducting states have been fitted, it is possible to extract the volume fraction of the insulating phase as a function of temperature, $V_s(T)$. This quantity acts as an effective order parameter with which to describe the transformation dynamics. At the same time, V_s can be correlated to the peak in $-d(\ln R)/dT$ as a function of T. In a percolative picture of the transition, this peak should signal the percolation threshold of the system, as described above. In Fig. 8 we have plotted $V_s(T)$ on cooling and heating for some $NdNiO_3$ films of standard thickness (~200 nm) grown on LAO. $-d(\ln R)/dT$ as a function of T has been plotted on the same axes. The plot indicates that the peak associated with T_{MI} corresponds to a volume ratio $V_s \sim 0.65$, i.e., a metallic ratio of $\sim\frac{1}{3}$, the predicted percolation threshold of a three-dimensional cubic lattice ($1/D$).

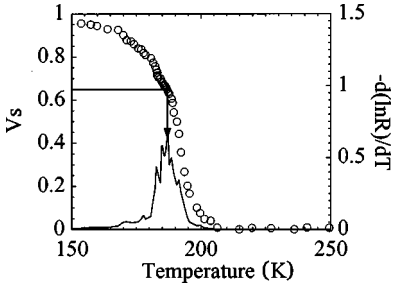

FIG. 9. Volume fraction of the insulating phase (circles) and $-d(\ln R)/dT$ (solid line) as a function of temperature for bulk ceramics (calculations performed on heating data extracted from Ref. 13). The result indicates that the coincidence between T_{MI} and the percolation threshold $V_s=\frac{2}{3}$ is a general feature of the metal-insulator transition of $NdNiO_3$.

This analysis can also be performed on bulk samples. The data reported for bulk $NdNiO_3$ (Ref. 13) has been fitted by the present authors following the procedure described above, and the corresponding T_{MI} has also been calculated as the peak in $-d(\ln R)/dT$. The results are plotted in Fig. 9. Again, the results indicate that T_{MI} corresponds to a volume fraction $V_s \sim \frac{2}{3}$.

The percolative model described is dimensionality sensitive: in the limit of a two-dimensional system, the percolation threshold should change from $\frac{1}{3}$ to $\frac{1}{2}$; consequently, T_{MI} should correspond to a volume ratio $V_s=\frac{1}{2}$. One would expect to observe a dimensional crossover in ultrathin films. Unfortunately, the thinner films grown on LAO cannot be used for this analysis: Figure 4 shows that for the thinner films grown on these substrates (16 and 8 nm), the hysteresis closes at very low temperatures (below 30 K for 16 nm, and less than 15 K for 8 nm). In these conditions it is not possible to obtain a meaningful fit of the semiconducting state, as the conductivity is dominated by pure VRH below 30 K, and consequently $V_s(T)$ cannot be calculated.

On the other hand, although thicker films grown on NGO display a double peak in $-d(\ln R)/dT$ (Fig. 5), the thinner samples (37 and 18 nm) show only one. When correlating this peak to V_s, it was found that T_{MI} evolved towards $V_s \sim \frac{1}{2}$ (Fig. 10). We interpret this apparent crossover thickness between three and two dimensions as an indication of the size ($\sim$15–20 nm) of the metallic and insulating regions in the mixed state of the nickelate films grown on NGO.

CONCLUSIONS

A study of the transport properties and MI phase transition behavior in as-grown $NdNiO_3$ thin films made by PLD was presented. dc conductivity was characterized as a function of substrate and film thickness, and differences were analyzed in terms of the effect of lattice mismatch-induced epitaxial strain on the films. The results were presented in two sections: Section I focused on the details of the growth study and the effect of epitaxial strain on the transition, and Sec. II aimed to give a more general insight into the transport properties and percolative phenomena of our films and previously published data for bulk. The main results from Sec. I are the following.

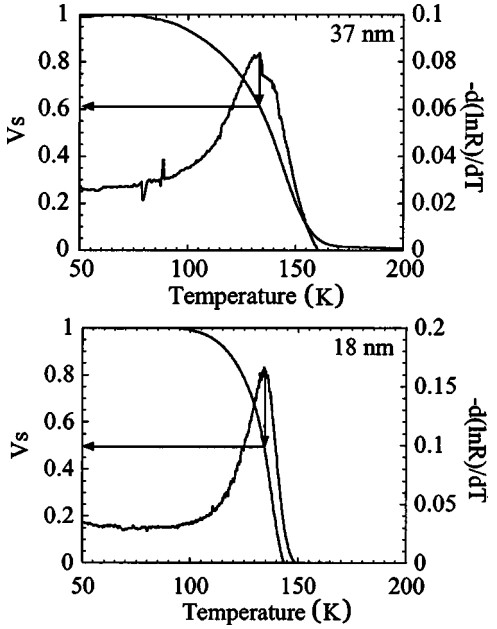

FIG. 10. $V_s(T)$ and $-d(\ln R)/dT$ as a function of temperature on heating for two thin films grown on NGO. The observed $V_s \cong \frac{1}{2}$ for the thinnest suggests a crossover toward 2D behavior. This crossover thickness ($\sim$15–20 nm) is interpreted as an indication of the size of the semiconducting and metallic clusters in the mixed state.

(i) Films grown on MgO are not epitaxial, and do not show any phase transition, being semiconducting at all measured temperatures.

(ii) Films grown on STO, NGO, and LAO are strongly oriented and display a distinct MI transition. The sharpness of the transition improves on substrates with a reduced lattice mismatch.

(iii) Both tensile and compressive epitaxial strains were observed to decrease T_{MI}, and reduce the resistance jump between the metallic and insulating phases. Tensile strain straightens the Ni-O-Ni bond angle, which increases the orbital overlap between O^{2-} and Ni^{3+}, thus closing the charge-transfer gap. For films grown on LAO, bond straightening can be rationalized in terms of an increase in the in-plane symmetry of the $NdNiO_3$ films.

Having established the differences between films grown on different substrates, in Sec. II the conductance behavior of the semiconducting regime was analyzed, and the phase transition itself was modeled using a percolative approach. The main results arising from this section are critically discussed and compared to those reported for bulk ceramics. The conclusions of Sec. II can be summarized in two points.

(i) The semiconducting state of $NdNiO_3$ can be fitted in the entire measured temperature range below T_{MI} by assuming that thermally activated conduction and Mott variable range hopping occur simultaneously. This result also seems to be a general feature of $NdNiO_3$ in bulk form. The coexistence of VRH and thermally activated conduction at relatively high temperatures is consistent with the strength of the electron-phonon interaction and the percolative nature of the transition in these compounds.

(ii) T_{MI} seems to correspond with the loss of metallic connectivity in a percolative lattice. For films thinner than ~18 nm grown on NGO, T_{MI} corresponds to the percolation threshold of a two-dimensional lattice ($V_s = \frac{1}{2}$). This was interpreted as an indication of the scale of the heterogeneity in the mixed state of $NdNiO_3$ films grown on these substrates.

ACKNOWLEDGMENTS

This project was partly funded by the EPSRC, the European Social Fund, NICAM, and The Royal Society. The authors wish to thank Dr. Martin McCurry for constructing the resistance measurement system, and the staff of the electron microscopy unit at QUB.

*Corresponding author. Electronic address:m.gregg@qub.ac.uk

[1] P. Lacorre, J. B. Torrance, J. Pannetier, A. I. Nazzal, P. W. Wang, and T. C. Huang, J. Solid State Chem. **91**, 225 (1991). For a review, see M. L. Medarde, J. Phys.: Condens. Matter **9**, 1680 (1997).

[2] P. C. Canfield, D. J. Thompson, S.-W. Cheong, and R. L. Rupp, Phys. Rev. B **47**, 12 357 (1993).

[3] X. Obradors, L. M. Paulius, M. B. Maple, J. B. Torrance, A. I. Nazzal, J. Fontcuberta, and X. Granados, Phys. Rev. B **47**, 12 353 (1993).

[4] M. Medarde, J. Mesot, P. Lacorre, S. Rosenkrantz, P. Fischer, and K. Gobretch, Phys. Rev. B **52**, 9248 (1995).

[5] M. Medarde, J. Mesot, S. Rosenkranz, P. Lacorre, W. Marshall, S. Klotz, J. S. Loveday, G. Hamel, S. Hull, and P. Radaelli, Physica B **234–236**, 15 (1997).

[6] J. L. García-Muñoz, J. Rodríguez-Carvajal, P. Lacorre, and J. B. Torrance, Phys. Rev. B **46**, 4414 (1992).

[7] J. A. Alonso, J. L. Garcia-Muñoz, M. T. Fernández, M. A. G. Aranda, M. J. Martíez-Lope, and M. T. Casais, Phys. Rev. Lett. **82**, 3871 (1999).

[8] J. B. Torrance, P. Lacorre, A. I. Nazzal, E. J. Ansaldo, and Ch. Niedermayer, Phys. Rev. B **45**, 8209 (1992).

[9] J. Zaanen, G. A. Sawatzky, and J. W. Allen, Phys. Rev. Lett. **55**, 418 (1985).

[10] X. Granados, J. Fontcuberta, X. Obradors, Ll. Mañosa, and J. B. Torrance, Phys. Rev. B **48**, 11 666 (1993).

[11] M. Medarde, P. Lacorre, K. Conder, F. Fauth, and A. Furrer, Phys. Rev. Lett. **80**, 2397 (1998).

[12] J. L. García-Muñoz, J. Rodríguez-Carvajal, and P. Lacorre, Phys. Rev. B **50**, 978 (1994).

[13] R. Mallik, E. V. Sampathkumaran, J. A. Alonso, and M. J. Martinez-Lope, J. Phys.: Condens. Matter **10**, 3969 (1998).

[14] I. Vobornik, L. Perfetti, M. Zacchigna, M. Grioni, G. Margaritondo, J. Mesot, M. Medarde, and P. Lacorre, Phys. Rev. B **60**, 8426 (1999).

[15] G. Demazeau, A. Marbeuf, M. Pouchard, and P. Hagenmuller, J. Solid State Chem. **3**, 582 (1971).

[16] J. K. Vassiliou, M. Hornbostel, R. Ziebarth, and J. F. Disalvo, J. Solid State Chem. **81**, 208 (1989).

[17] J. García, A. González, M. J. Sanchis, M. D. Marcos, E. Martínez, F. Sapiña, D. Beltran, and A. Beltran, Solid State Ionics **63-65**, 52 (1993).

[18] J. F. DeNatale and P. H. Kobrin, J. Mater. Res. **10**, 2992 (1995).

[19] G. Catalan, R. M. Bowman, and J. M. Gregg, J. Appl. Phys. **87**, 606 (2000).

[20] S. Metev, in *Pulsed Laser Deposition of Thin Films*, edited by D. B. Chrisey and G. K. Hubler (Wiley, New York, 1994).

[21] *Handbook of Chemistry and Physics*, edited by R. C. Weast (CRC Press, Cleveland, OH, 1974), Vol. E68.

[22] A. Tiwari and K. P. Rajeev, Solid State Commun. **109**, 119 (1999).

[23] R. Mahesh, K. R. Kannan, and C. N. R. Rao, J. Solid State Chem. **114**, 294 (1995).

[24] M. E. Fisher and J. S. Langer, Phys. Rev. Lett. **20**, 665 (1968).

[25] J. Pérez-Cacho, J. Blasco, J. García, M. Castro, and J. Stankiewitz, J. Phys.: Condens. Matter **11**, 405 (1999).

[26] J. W. Mathews and A. E. Blackeslee, J. Cryst. Growth **27**, 118 (1974).

[27] L. B. Freund and W. D. Nix, Appl. Phys. Lett. **69**, 173 (1996).

[28] P. A. Langjahr, F. F. Lange, T. Wagner, and M. Ruhle, Acta Mater. **46**, 773 (1997).

[29] K. Hayashi, G. Demazeau, and M. Pouchard, Rev. Chim. Miner. **18**, 148 (1981).

[30] A. Kar Gupta and A. K. Sen, Phys. Rev. B **57**, 3375 (1998).

[31] N. Mott, *Metal-Insulator Transitions* (Taylor & Francis, London, 1974).

[32] R. D. Sánchez, M. T. Causa, A. Caneiro, A. Butera, M. Vallet-Regí, M. J. Sayagués, J. González-Calbet, F. García-Sanz, and J. Rivas, Phys. Rev. B **54**, 16 574 (1996).

[33] T. G. Castner, in *Hopping Transport in Solids*, edited by M. Pollak and B. Shklovskii (Elsevier, Amsterdam, 1991).

[34] M. Medarde, P. Lacorre, K. Conder, J. Rodríguez-Carvajal, S. Rosenkrantz, F. Fauth, and A. Furrer, Physica B **241-243**, 751 (1998).

[35] N. E. Massa, J. A. Alonso, M. J. Martínez-Lope, and I. Rasines, Phys. Rev. B **56**, 986 (1997); M. A. Mogrinski, N. E. Massa, Horacio Salva, J. A. Alonso, and M. J. Martínez-Lope, *ibid.* **60**, 5304 (1999).

[36] D. Emin, Phys. Rev. Lett. **32**, 303 (1974).

[37] M. Pollak, M. L. Knotek, H. Kurtzman, and H. Glick, Phys. Rev. Lett. **30**, 856 (1973).